In-plane displacement measurement in vortex metrology by synthetic network correlation fringes

Luciano Angel-Toro,[1,*] Daniel Sierra-Sosa,[1,2] Myrian Tebaldi,[2] and Néstor Bolognini[2,3]

[1]*Grupo de Óptica Aplicada, Departamento de Ciencias Básicas, Universidad EAFIT, Medellín (7023), Colombia*
[2]*Centro de Investigaciones Ópticas, CIOp [Centro Científico Tecnológico La Plata - Consejo Nacional de Investigaciones Científicas Técnicas, Comisión de Investigaciones Científicas (CONICET, CIC)] and OPTIMO Departamento Ciencias Básicas, Facultad Ingeniería, Universidad Nacional de La Plata (UNLP)], P.O. Box 3 (1987), M. B. Gonnet, Argentina*
[3]*Facultad de Ciencias Exactas, Universidad Nacional de La Plata, La Plata, Argentina*
**Corresponding author: langel@eafit.edu.co*

Received October 10, 2012; revised January 17, 2013; accepted January 17, 2013;
posted January 18, 2013 (Doc. ID 177822); published February 21, 2013

Recently we proposed an alternative method of displacement analysis in vortex metrology, based on the application of the Fourier optics techniques, that is suitable for an intermediate range of displacement measurements ranging below the resolution of speckle photography and above that of the conventional vortex metrology. However, for smaller displacements, we introduce an approach to perform the Fourier analysis from vortex networks. In this work, we present an enhanced method for measuring uniform in-plane displacements, taking advantage of the capability of determining the subpixel locations of vortices and having the ability to track the homologous vortices onto a plane. It is shown that high-quality fringe systems can be synthesized and analyzed to accurately measure in an extended range of displacements and for highly decorrelated speckle patterns. Experimental results supporting the validity of the method are presented and discussed.

OCIS codes: 050.4865, 030.6140.

1. INTRODUCTION

In speckle photography, for rigid in-plane displacements Young's fringes are formed whose period and direction are related to the speckle displacements [1–5]. There, speckles allow tracking of the local displacement onto a coherently illuminated surface. Similarly, in vortex metrology, vortices associated with speckle distributions can be used as markers imprinted onto the surface, which allow for measurement of global and local subspeckle displacements onto the diffusing surface. In [6] the effect of speckle decorrelation on the reliability of the results obtained by using conventional algorithms for in-plane displacements analysis in vortex metrology was studied. In particular, it was shown that the quality of histograms depicting the relative coordinate displacements between homologous vortices in general decreases. Indeed, when processing the histograms, wider distributions are obtained for decorrelated speckles than for undecorrelated ones. Also, a significant reduction in the certainty of measurements is of concern in the decorrelated speckle case. Motivated by these facts, in [7] a method based on the application of the Fourier techniques in vortex metrology that allows measuring of relative displacements by using decorrelated speckle distributions was presented. This method is able to measure in a range where both optical vortex metrology and speckle photography are prone to failure. To study the magnitude and orientation of the relative displacements between pairs of homologous vortices onto a plane, the authors use the fast Fourier transform (FFT) algorithm to produce systems of Young's fringes to be interpreted in terms of diffraction patterns generated by means of masks containing multiple apertures at the approximate vortex locations. Although in that work the vortices are located with subpixel precision, this information is not taken into account when replacing vortex locations with one-pixel apertures. As a consequence, a lack of resolution is of concern. Moreover, although the correlation fringes obtained by using this method [7] allow for studying the in-plane displacements, it is apparent that the speckle noise deteriorates the fringes quality, and their visibilities do not reach the optimum, even if a smoothing filter was applied. This obviously lowers the measurement accuracy by incrementing the respective variances.

To overcome these constraints, in this work an alternative way to carry out the Fourier analysis from vortex networks is presented and discussed. The method is summarized as follows. Two speckle patterns are successively recorded, each of them associated with a different state of a diffuser, before and after a uniform in-plane displacement. Afterward, the recorded images are processed by using a series of digital tools, starting with the use of standard algorithms, frequently employed in vortex metrology, and ending with a tool based on a strategy for processing the information on the location and pairing of vortices, according to their core structure properties. Specifically, after recording, each image is digitally processed to generate an analytic signal by means of the Riesz transform. Then, by using this transform, we associate each of the intensity recordings with a corresponding bidimensional pseudo-phase map containing vortices [8]. These vortices are located with subpixel resolution and paired as homologous vortices [9–11]. Afterward, in our approach a non-conventional technique is implemented to associate a synthetic fringe system with each pair of homologous vortices and, overlapping all the resulting systems, is to be analyzed. It

is shown that high-visibility fringes allow for accurate measuring in an extended range of displacements, even when the speckle decorrelation is of concern. In Section 2, the theoretical approach sustaining this proposal is elaborated, and in Section 3, some results are presented and analyzed. This analysis includes a comparison of the accuracy and the application range of our results in relation with those first introduced by Wang *et al.* in [9,10] and those presented in our previous work [7]. This provides an idea about the improvement proposed in this paper.

2. THEORETICAL APPROACH

In the Fraunhofer regime, except from the phase factors that are not of interest when evaluating the output intensity, the scalar diffracted field can be associated with a rescaled Fourier transform applied to the complex field existing at the entrance pupil by using the paraxial approximation [12]:

$$U_2(x,y)=\frac{1}{\lambda z}\iint_{-\infty}^{\infty}U_1(\xi,\eta)\left[e^{\frac{-ik}{z}(x\xi+y\eta)}\right]\mathrm{d}\xi\mathrm{d}\eta, \tag{1}$$

where $U_1(\xi,\eta)$ and $U_2(x,y)$ represent the input and output complex signals, respectively, λ is the illuminating wavelength, $k=2\pi/\lambda$ is the wavenumber, and z represents the propagation distance from the input to the output plane, satisfying the far-field condition $z\gg(\pi/\lambda)(\xi^2+\eta^2)_{\max}$.

In Fig. 1 a scheme representing the input and diffraction planes and their respective coordinate systems is presented.

To start, let us consider a diffracted field associated with a set of N ideal individual radiators (or apertures) located onto the input plane, at points that correspond to the actual positions of vortices onto the phase maps, before and after displacement. By doing this, the complex amplitude onto the observation plane can be obtained from the coherent superposition of waves coming from the individual radiators, as follows:

$$A(x,y)=\sum_{i=1}^{N}A_i(x,y), \tag{2}$$

where N is the number of apertures and $A_i(x,y)$ represents the complex field amplitude that propagates from the ith aperture at point (ξ_i,η_i) up to a generic point (x,y) at the observation plane. Then the corresponding intensity $|A(x,y)|^2$ onto the observation plane is given by

$$I(x,y)=NI_0+2I_0\sum_{\substack{i,j=1\\ i<j}}^{N}\cos[\varphi_j(x,y;\xi_j,\eta_j)-\varphi_i(x,y;\xi_i,\eta_i)], \tag{3}$$

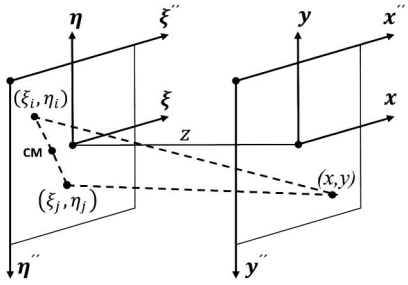

Fig. 1. Scheme representing the input and diffraction planes, including the different axes and coordinate systems introduced in the text.

where I_0 is the intensity associated with an individual aperture, and $\varphi_i(x,y;\xi_i,\eta_i)$, for $i=1,2,\ldots N$, represents the phase of the wave going from (ξ_i,η_i) at the input plane to (x,y) at the output plane. By following Fig. 1 and assuming that waves at the input plane are synchronous, under the paraxial approximation,

$$\varphi_i(x,y;\xi_i,\eta_i)\approx\varphi_0+\frac{2\pi}{\lambda}\left\{z+\frac{1}{2z}[(x-\xi_i)^2+(y-\eta_i)^2]\right\}, \tag{4}$$

where φ_0 is a constant representing the common phase of waves emerging from the (ξ,η) plane.

By combining Eqs. (3) and (4):

$$I(x,y)=NI_0+2I_0\sum_{\substack{i,j=1\\ i<j}}^{N}\cos\left\{\frac{\pi}{\lambda z}[(\xi_j^2+\eta_j^2)-(\xi_i^2+\eta_i^2)]-\frac{2\pi}{\lambda z}[(\xi_j-\xi_i)x+(\eta_j-\eta_i)y]\right\}. \tag{5}$$

This equation implies that the intensity of the diffracted field (as the intensity associated with the Fourier transform) corresponding to the apertures onto the input plane can be synthesized as the incoherent superposition of a DC term (resulting from the addition of the individual contributions of the apertures) and a series of fringe systems associated with the interference of all the different pairs of apertures in the same plane [13].

It should be noted that there is a contribution for any pair of apertures, no matter whether the pair of apertures corresponds to two homologous vortices or not. Nevertheless, because of the redundancy in the distance and relative orientation of the homologous vortex pairs, also in this case, a system of correlation fringes can be observed onto the diffraction plane whose spatial frequency is related with the displacement between the speckled images [7].

However, the only relevant information in our analysis is that corresponding to the relative displacements between the pairs of homologous vortices. Then, according to our purpose, all those interference terms in Eq. (5) related with nonhomologous vortex pairs should be removed. In summary, we are interested only in those cosine terms that reveal the relative displacement redundancy. It should be highlighted that this operation cannot be achieved by using a conventional optical processor, as in the case of implementing a Fourier transform. Therefore, we must perform this procedure by means of numerical calculations. By removing all the cosine contributions corresponding to pairs of nonhomologous vortices, from Eq. (5) it follows that the intensity distribution of interest is

$$I'(x,y)=I_0\left[N'+\sum_{\substack{i,j=1\\ i<j}}^{N'}\cos\left\{\frac{\pi}{\lambda z}[(\xi_j'^2+\eta_j'^2)-(\xi_i'^2+\eta_i'^2)]-\frac{2\pi}{\lambda z}[(\xi_j'-\xi_i')x+(\eta_j'-\eta_i')y]\right\}\right], \tag{6}$$

where N' represents the total number of homologous vortex pairs contributing to fringe formation, each of them constituted by vortices associated with different states of the diffuser, before and after displacements. Thus, the summation

extends over all these pairs whose locations are denoted by using the primed coordinates (ξ_i', η_i') and (ξ_j', η_j'), respectively. In the following we will call the "center" of such a pair the point in the middle of the line connecting the two vortices, which is located at $(1/2)(\xi_j' + \xi_i', \eta_j' + \eta_i')$.

Note that the effect of the first term of the cosine argument in Eq. (6) is to change, in a selective way, the phase of the individual fringes contributing to the intensity, or, equivalently, it moves the position of each individual fringe system from the origin of the reference system to a point located just in front of the center of the corresponding pair of vortices. Nevertheless, for analyzing the relative displacement between the different pair of homologous vortices, the position of the individual pairs is not really relevant. Accordingly, we displace the center of all the pairs of homologous vortices from their original locations to the origin of the coordinate system so that all the individual fringe systems coincide at the center of the observation plane. Thus, we focus the attention in measuring the relative displacement between two correlated vortex networks, not on the specific locations of the different pairs of homologous vortices. Consequently, the locations of the homologous vortices at (ξ_i', η_i') and (ξ_j', η_j') are redefined as $(\tilde{\xi}_i, \tilde{\eta}_i) = (1/2)(\xi_i' - \xi_j', \eta_i' - \eta_j')$ and $(\tilde{\xi}_j, \tilde{\eta}_j) = (1/2)(\xi_j' - \xi_i', \eta_j' - \eta_i')$, respectively. Then the intensity distribution of interest is

$$I''(x,y) = I_0\left[N' + \sum_{\substack{i,j=1\\ i<j}}^{N'} \cos\left\{\frac{2\pi}{\lambda z}[(\tilde{\xi}_j - \tilde{\xi}_i)x + (\tilde{\eta}_j - \tilde{\eta}_i)y]\right\}\right]$$
$$\propto \frac{1}{2} + \left(\frac{1}{2N'}\right)\sum_{\substack{i,j=1\\ i<j}}^{N'} \cos\left\{\frac{2\pi}{\lambda z}[(\tilde{\xi}_j - \tilde{\xi}_i)x + (\tilde{\eta}_j - \tilde{\eta}_i)y]\right\}. \tag{7}$$

Note that, from this equation, if follows that $0 \le I''(x,y) \le 1$.

Finally, we have to consider that the images are represented by $m \times n$ matrices, and when calculating the output intensity by using computational algorithms, we start computing from the upper-left corner corresponding to the matrix element (1,1), and then we proceed from left to right and from top to bottom, up to reach the matrix element (m,n). Accordingly, we have to change the coordinate system to a new one whose origin corresponds to the (1,1) matrix element. The new set of coordinates at the input (ξ_i'', η_i'') and the output (x'', y'') planes are defined by the transformations $(\xi_i'', \eta_i'') = ((n/2) + \tilde{\xi}_i, (m/2) - \tilde{\eta}_i)$ and $(x'', y'') = ((n/2) + x, (m/2) - y)$, respectively. It leads to the final expression for the output intensity we are interested in:

$$I''(x'', y'') = \frac{1}{2} + \frac{1}{2N'}\sum_{\substack{i,j=1\\ i<j}}^{N'} \cos\left\{\frac{2\pi}{\lambda z}\left[(\xi_j'' - \xi_i'')\left(x'' - \frac{n}{2}\right)\right.\right.$$
$$\left.\left. + (\eta_j'' - \eta_i'')\left(y'' - \frac{m}{2}\right)\right]\right\}. \tag{8}$$

Note that the factor $\kappa = \lambda z$ in the cosine argument can be set to any convenient value in order to rescale the period of the fringe systems contributing to the intensity distribution. Besides, this allows for settling the average number of pixels per fringe. The period of an elemental fringe system associated with a pair of homologous vortices located at (ξ_i'', η_i'') and (ξ_j'', η_j'') is given by

$$\Lambda_{ij} = \lambda z[(\xi_j'' - \xi_i'')^2 + (\eta_j'' - \eta_i'')^2]^{-\frac{1}{2}}. \tag{9}$$

Also, it should be highlighted that, by using Eq. (8) for depicting the incoherent superposition of the fringe systems of interest, we can use the information on the highly accurate localization of vortices on the basis of determining their relative in-plane displacements with subpixel resolution.

3. EXPERIMENTAL RESULTS AND DISCUSSION

A. Setups for Recording

The experimental arrangement for recording the speckled images are presented in Fig. 2. Two speckled images are recorded before and after a diffuser displacement. An He–Ne (633 nm) collimated laser beam impinges onto an opaque mask with a circular aperture, which is located immediately behind the mask. Then objective speckles are formed at a distance z apart from the diffuser. A CMOS camera is used for recording. We set $z = 820$ mm and the aperture's diameter to 5 mm, which implies that the transversal average speckle size onto the observation plane is 126.6 μm. In the arrangement of Fig. 2(a) the mask and the diffuser are moved jointly; therefore, the same set of radiators generates the speckles before and after displacement, and no decorrelation occurs between images. In Fig. 2(b) the diffuser is moved while the mask remains fixed. Then the illuminated area onto the diffuser changes as the diffuser moves between recordings, leading to changes into the speckle distributions. Thereby,

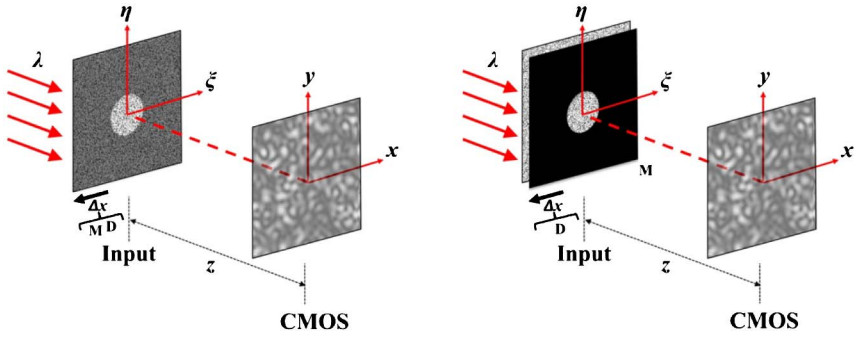

Fig. 2. (Color online) Experimental arrangements for recording the speckled images before and after an in-plane displacement for (a) undecorrelated and (b) decorrelated speckle patterns. λ, wavelength; D, diffuser; M, mask; CMOS, camera; Δx, in-plane displacement.

in this case the speckle fields decorrelate by the effect of the movement of radiators over the aperture. Even though the decorrelation effect could not have significant influence for small displacements, its effect becomes apparent as far as the displacement increases.

B. Synthetic Vortex Correlation Fringes

In this section we present and discuss some representative experimental results supporting our proposal. As mentioned before, two digital speckled images for the initial and final state of the diffuser are recorded. The original format of each recorded image is 2352×1728 pixels in size, and speckles are undecorrelated or decorrelated according to the setup of Fig. 2 that, according to the case, is employed. Each speckled image is processed to generate an analytic signal by means of a digital version of the Riesz transform. The integral form of Riesz transform is [8]

$$\tilde{I}(x,y) = \iint_{-\infty}^{\infty} V(f_x,f_y)\mathcal{F}(f_x,f_y)e^{2\pi i(f_x x+f_y y)}\mathrm{d}f_x f_y, \qquad (10)$$

where $\mathcal{F}(f_x,f_y)$ is the Fourier transform of the intensity distribution of the speckle pattern after the subtraction of its mean value and $V(f_x,f_y)$ is the spiral phase function given by

$$V(f_x,f_y) = e^{i\,\arctan(f_y/f_x)}. \qquad (11)$$

Then, by using this transform, we can assign a bidimensional pseudo-phase map containing vortices to each intensity recording. Although the Laguerre–Gauss transform [9,10] has advantages in comparison with the Riesz transform, such as optimally distributed phase singularities, high-frequency noise reduction that prevents unstable vortices, and control over the density of singularities, we employed the Riesz transform for our convenience, aimed to reduce the number of parameters involved in experiments. This election has no special relevance in this context because our method consists of an alternative way to process the vortex networks information once they have been obtained from the intensity recordings. Vortices onto each pseudo-phase map are located with subpixel resolution as in [9] and paired as homologous vortices as in [10]. Each pair by definition must be composed of vortices having the same topological charge and very similar core structure parameters (eccentricity, real and imaginary components, zero crossing angle, vorticity). Then the coordinate displacements Δx and Δy corresponding to the different homologous pairs are determined. To move forward, instead of the usual procedure, we follow the procedure introduced in Section 2. Specifically, to each pair of homologous vortices, we define an individual system of interference fringes, equivalent to one generated by a pair of synchronous point radiators, whose separation and relative orientation remain the same, but symmetrically located with respect to the center of the recording plane. Finally, all these fringe systems are added as intensity patterns.

In Table 1, two fringe patterns, generated by following this procedure, and their corresponding intensity profiles are presented. Both fringe patterns are obtained for equal

Table 1. Effect of Decorrelation on Synthetic Vortex Correlation Fringe Visibility[a]

Undecorrelated speckle	*Decorrelated speckle*
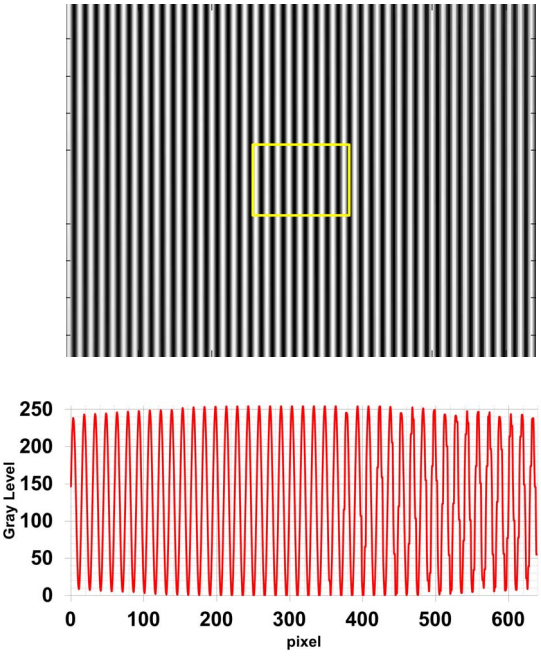	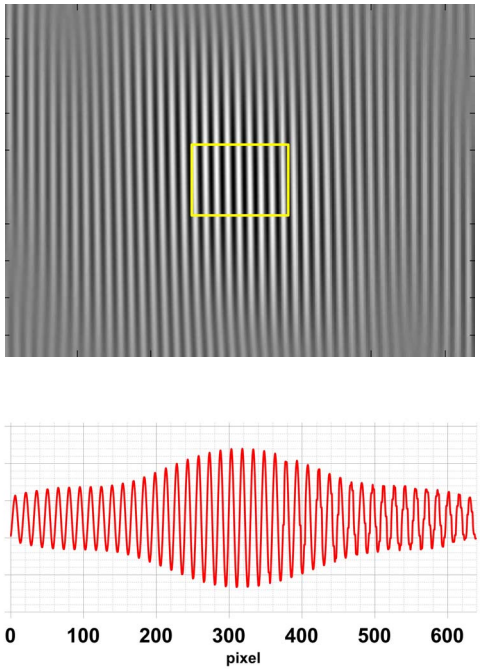

[a]Fringes correspond to (a) undecorrelated and (b) decorrelated speckled images recorded by using the setups of Figs. 2(a) and 2(b), respectively. In both cases the same displacement of $\Delta x = 16$ μm along the horizontal axis is produced during recording, and the same scale factor $\lambda z = 30$ pixels^2 is employed.

displacements of $\Delta x = 16$ μm along the horizontal axis ($\Delta y = 0$) and by using the same scale factor $\lambda z = 30$ pixels^2. To obtain the results of the left column, the setup of Fig. 2(a) is employed; then decorrelation is not of concern except for that produced by the flow of vortices in or out of the pseudo-phase maps when the diffuser is moved. In the right column, the results generated by using the setup in Fig. 2(b) are presented, which implies that, in this case, the decorrelation is involved. Note that fringe visibility approaches unity at the center of the fringe systems, where all the fringes position coincides. However, it is apparent that fringe visibility decreases from the center to the edges. This is because the periods and relative orientations of the overlapped fringe systems do not exactly coincide, given that the distances and relative orientation of homologous vortex pairs onto the pseudo-phase maps, although very similar, are not the same. Thus, as decorrelation increases, the region of high-quality fringes decreases.

For measuring proposals, the relevant magnitudes in the results are associated with the fringe period and orientation. Specifically, the average period $\langle\Lambda\rangle$ and the average angle $\langle\theta\rangle$ between the fringes and the vertical y axis as well as the respective variances σ_Λ^2 and σ_θ^2 of these magnitudes are of interest. In Table 2, the measured values for the results of Table 1 are presented. Note that, in the decorrelated case, the number of pairs of homologous vortices decreases to as low as 3.7% with respect to the undecorrelated case, which in turn implies a reduction in the certainty of measurements for displacements. Note that, in both cases, the average displacement $\langle\Delta x\rangle$ between homologous vortices approaches 2 pixels, which is the expected value for an actual 16 μm displacement in our experiments. However, a higher accuracy is achieved if decorrelation is not of concern. To determine the average fringe period $\langle\Lambda\rangle$ and its variance σ_Λ^2, the values of the periods of the individual fringe systems, for the different pairs of homologous vortices, are separately calculated. The values corresponding to $\langle\theta\rangle$ and σ_θ^2 are evaluated by following a similar procedure. As expected, although in both cases $\langle\Lambda\rangle$ approaches the expected value $\Lambda = (\lambda z/\Delta x) = 15$ pixels, the respective variance is several orders of magnitude lower in the case of the undecorrelated speckles. Similarly, note that $\langle\theta\rangle$ can be approximated to zero in both cases, but the variance σ_θ^2 for the undecorrelated speckles is quite lower than in the decorrelated case, affecting the certainty in measurements.

An important feature of our method is that, by properly selecting the scale factor λz, the fringe visibility can be improved in order to reach the optimum anywhere the fringes are depicted. It allows us to obtain both the best discrimination of periods and relative orientation of fringes. Moreover, by means of an adequate selection of the scale parameter, it is possible to enlarge the images with no associated pixilation. These effects are shown in Table 3, obtained by processing the same images as in Table 1, using a different scale parameter. Fringes depicted in the left and right columns of Table 3 correspond to enlarged versions of fringes inside the region marked in the respective columns in Table 1. It is apparent that, in both cases, no matter the decorrelation of speckles, high-visibility fringes can be achieved to accurately measure the respective periods and orientations and, on this basis, to determine the coordinate components of in-plane displacements.

In Table 4 it is shown that, as expected, when using the same scale factor, the spatial frequency of fringes increases proportionally to the displacement between images. In fact, the average spatial frequency of fringes in the right column of Table 4, for a 160 μm displacement, is twice the spatial frequency observed in the left column, corresponding to a 80 μm displacement.

On the other hand, the effect of changing the magnitude of displacements can be compensated by choosing a different scale factor, as is inferred from a comparison of fringes in the right column of Table 3 and in the left column of Table 4. In both cases the ratio between the scale factor and displacement is $(\lambda z/\Delta x) = (150\ \text{pix}^2/16\ \mu\text{m})$.

Table 2. Undecorrelated and Decorrelated Data Synthesis

	Undecorrelated Speckle	Decorrelated Speckle
Number of Homologous Vortex Pairs	2369	88
$\langle\Delta x\rangle$ (pixels)	1.9986	1.9830
σ_x^2 (pixels^2)	0.0035	0.0569
$\langle\Delta y\rangle$ (pixels)	0.0002	0.0033
σ_y^2 (pixels^2)	0.0019	0.0571
$\langle\Lambda\rangle$ (pixels)	15.0039	15.0234
σ_Λ^2 (pixels^2)	0.0214	0.0767
$\langle\theta\rangle$ (rad)	0.4187	0.4133
σ_θ^2 (rad^2)	$1.4763 \cdot 10^{-5}$	$6.2207 \cdot 10^{-5}$

C. Accuracy and Application Ranges of Measurement

To allow a comparison of the accuracy and the range of application of the method and also to bring an idea about the value of the improvement proposed in this paper, we present a series of measurements analyzed by using both the present method, those methods presented in [7], and those by Wang *et al.* in [9,10]. We used the setup of Fig. 2(b) for recording and applied shifts with a fixed 8 μm step along the x axis between images. In these experiments the decorrelation effect is implied.

In Fig. 3(a) the results for measured diffuser displacements (in pixels) by using the conventional vortex metrology tools [9,10] are depicted. The zero-crossing line satisfying the least-squares criterion in this figure is $\Delta x(\text{pixels}) = [0.1256\ (\text{pixels}/\mu\text{m})]\Delta x(\mu\text{m})$, corresponding to the camera's 8 μm pixel width. Given that the speckle decorrelation significantly affects the quality of results as the displacement increases [6], in practice we found this method to be suitable for displacements up to 48 μm. To go further, we proceed by using the methods we implemented [7].

In Fig. 3(b) we present a series of measured average periods of the synthetic correlation fringes obtained by following this paper proposal. In this case, we use a scale factor $\lambda z = 600$ pixels^2 to optimize the fringe visibility for lateral displacements from 8 to 144 μm. The curve represents the theoretical behavior given by the hyperbola $\langle\Lambda\rangle(\text{pixels}) = (4800\ \mu\text{m} \cdot \text{pixels})(\Delta x(\mu\text{m}))^{-1}$. It is apparent that the experimental data match the expected behavior in this displacement range. For larger displacements we are in the speckle photography regime, given that the average speckle transversal dimension is about 127 μm.

Table 3. Enlarged Synthetic Vortex Correlation Fringes and Their Corresponding Intensity Profiles by Setting a Different Scale Factor[a]

Undecorrelated speckle	*Decorrelated speckle*
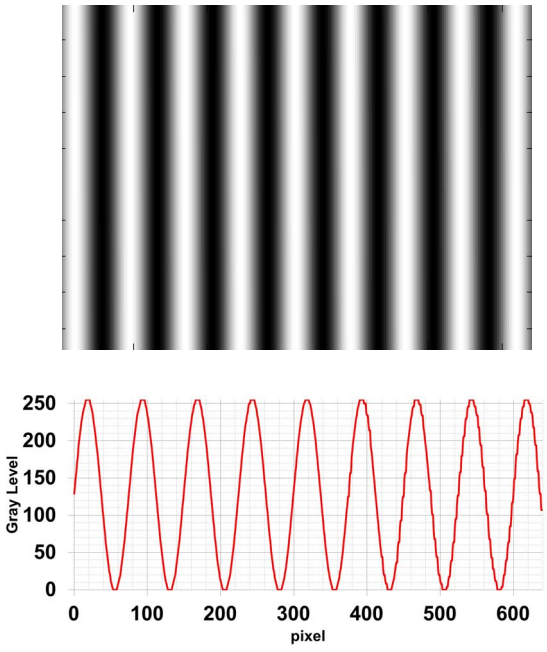	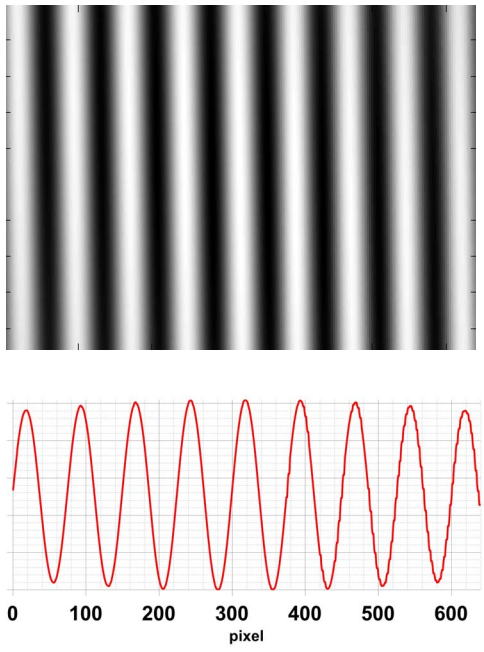

[a]Fringes are generated as in Table 1, for a 16 μm displacement, but in this case with a scale factor set at $\lambda z = 150$ pixels^2.

Table 4. Synthetic Vortex Correlation Fringes and Their Intensity Fringe Profiles for Two Different Horizontal Displacements[a]

80 μm	160 μm
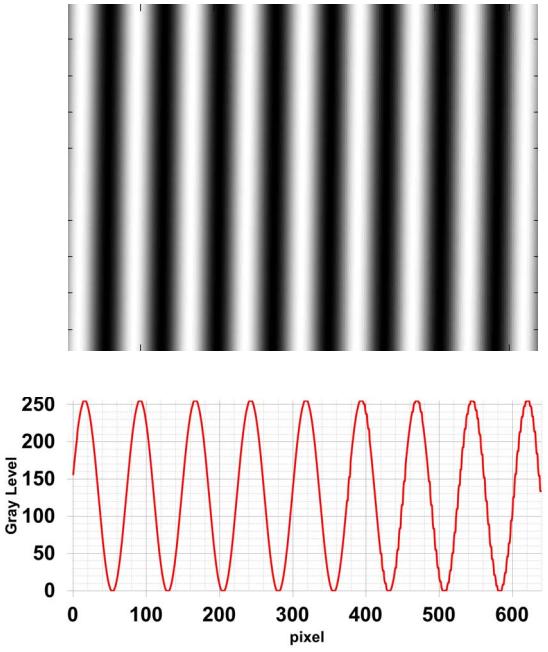	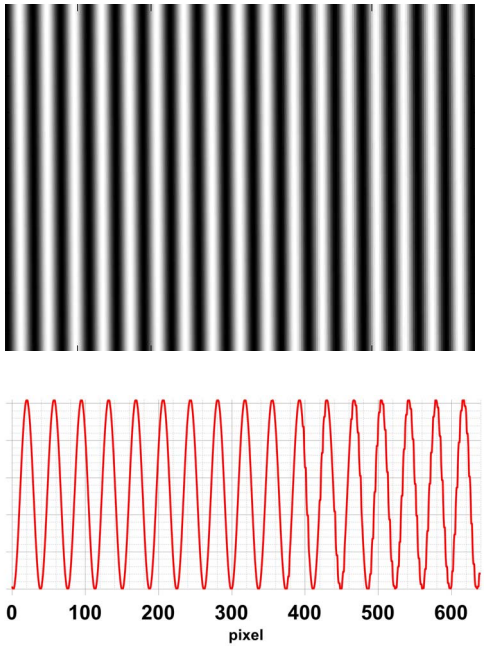

[a]In both cases the effect of decorrelation is of concern. The magnitude of displacement is 80 μm in the left column and 160 μm in the right column. Below each fringe pattern the respective intensity profile is depicted. In both cases the scale factor was set at $\lambda z = 750$ pixels^2.

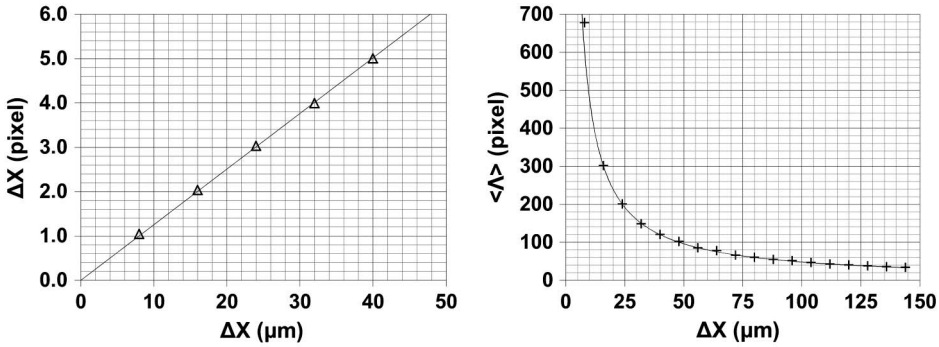

Fig. 3. (a) Measured displacements obtained by using the conventional information processing methods from vortex metrology. (b) Measured average periods of synthetic correlation fringes by following the method presented in this paper, with $\lambda z = 600$ pixels^2.

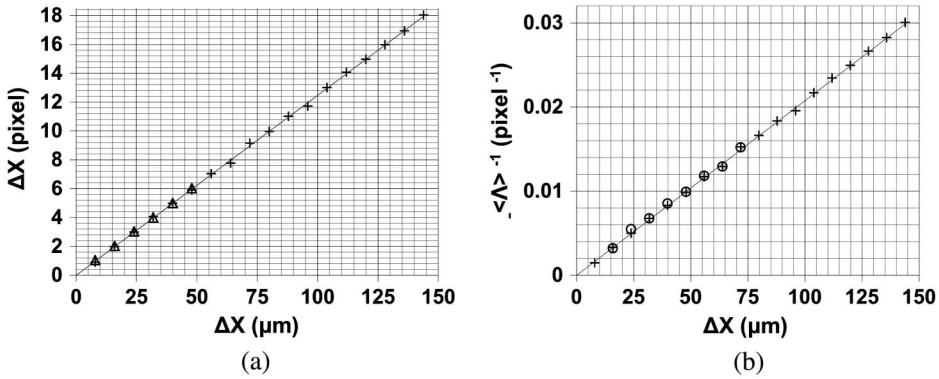

Fig. 4. (a) Measured displacements by using both the synthetic vortex correlation fringes from [7] (crosses) and the method introduced by Wang *et al.* in [9,10] (triangles). (b), the results obtained by means of both the vortex correlation fringes method [7] (circles) and by using the synthetic vortex correlation fringes method (crosses) presented in this paper.

In Fig. 4(a) the displacements evaluated on the basis of the data of Fig. 3(b) are presented (crosses). Also, the measured values for displacements in Fig. 3(a) by using the conventional vortex metrology [9,10] are depicted (triangles) to allow a comparison between the results obtained by using both methods. The line represents the same theoretical behavior of Fig. 3(a). Even though the experimental results related with both methods match with this behavior, it should be highlighted that those results obtained with the synthetic vortex correlation fringes allow for measuring in a wider range, up to the speckle photography regime.

To compare the results from our previous work [7] with those from this paper, Fig. 4(b) depicts a graph of the period inverse versus the displacement. The crosses represent experimental data corresponding to Fig. 3(b), and the circles apply for the results obtained on the basis of the Fourier method first introduced in [7]. In this case, the line for the theoretical behavior that is depicted is $\langle\Lambda\rangle^{-1}(\text{pixels}^{-1}) = (0,00021\ \mu\text{m}^{-1}\,\text{pixels}^{-1})\Delta x(\mu\text{m})$. Although in both cases there exists a good agreement between the experimental data and the theoretical predicted values, in the former technique [7], a narrower measurement range is of concern. In fact, this technique is unable to measure displacements below the dimension of 2 pixels because of the overlapping of the individual one-pixel apertures [7]. Also, for larger displacements, the presence of fringe systems related with nonhomologous vortex pairs and the influence of speckle noise in the Fourier transform diminish the vortex correlation fringe visibility. In our case, we obtained suitable fringe systems for measurements in an intermediate range up to 72 μm.

4. CONCLUSIONS

In this work, we take advantage of the subpixel localization of vortices onto the pseudo-phase maps for recorded speckles, before and after displacements, and a method to generate synthetic Young's fringe systems associated with displacements is proposed. These systems are obtained by means of an incoherent superposition of multiple individual fringe systems, each one associated with the interference of light coming from a different pair of point radiators, whose positions are determined by the homologous vortex location. The proposed method allows us to accurately measure in an extended range of displacements, in comparison with conventional vortex metrology when speckle decorrelation is of concern.

In comparison with the method proposed in [7], for measuring in-plane displacements from recorded speckle patterns, in the present proposal the accuracy is increased given that we use the information on the vortices subpixel location, the speckle noise affecting the quality of fringes is not of concern, and the contributions from fringe systems related with nonhomologous vortex in the Fourier transform are avoided. Moreover, disregarding restrictions arising from the overlapping of the individual one-pixel apertures, it is possible to measure lower magnitude displacements.

As is known, the effects associated with speckle decorrelation impose some constraints when using techniques for uniform in-plane displacement analysis in the context of conventional vortex metrology [6]. However, the method we have proposed in this paper is not restricted to the study of relative displacements between undecorrelated speckle patterns. By using this method, even though the fringe visibility decreases from center to edge of the fringe system as the decorrelation increases, it is possible to properly increase the fringe visibility by rescaling the fringe's period when setting the scale factor $\kappa = \lambda z$ into the cosine argument. Indeed, we have presented experimental evidences to support that, under the restrictions imposed by the speckle decorrelation, our proposal allows us to obtain high-visibility fringes. The latter allows for accurate measurement even if the decorrelation is of concern.

ACKNOWLEDGMENTS

Luciano Angel-Toro acknowledges Universidad EAFIT (Colombia) and financial support under the Academy of Sciences for the Developing World (TWAS)—United Nations Educational, Scientific, and Cultural Organization (UNESCO) Associateship Scheme at Centres of Excellence in the South for visiting the Centro de Investigaciones Opticas at La Plata, Argentina in 2011. This research was performed under Consejo Nacional de Investigaciones Científicas Técnicas grant no. 112-200801-00863 (Argentina) and Facultad de Ingeniería, Universidad Nacional de La Plata grant no. 11/I168 (Argentina).

REFERENCES

1. R. P. Khetan and F. P. Chiang, "Strain analysis by one-beam laser speckle interferometry. 1: single aperture method," Appl. Opt. **15**, 2205–2215 (1976).
2. F. P. Chiang and R. P. Khetan, "Strain analysis by one-beam laser speckle interferometry. 2: multiaperture method," Appl. Opt. **18**, 2175–2186 (1979).
3. L. Angel-Toro, M. Tebaldi, N. Bolognini, and M. Trivi, "Speckle photography with different pupils in a multiple-exposure scheme," J. Opt. Soc. Am. A **17**, 107–119 (2000).
4. L. Angel-Toro, M. Tebaldi, and N. Bolognini, "Multiple-aperture speckle method applied to local displacement measurements," Opt. Commun. **274**, 23–31 (2007).
5. L. Angel, M. Tebaldi, and N. Bolognini, "Multiple rotation assessment through isothetic fringes in speckle photography," Appl. Opt. **46**, 2676–2682 (2007).
6. L. Angel-Toro, D. Sierra-Sosa, M. Tebaldi, and N. Bolognini, "Speckle decorrelation influence on measurements quality in vortex metrology," Opt. Commun. **285**, 4312–4316 (2012).
7. L. Angel-Toro, D. Sierra-Sosa, M. Tebaldi, and N. Bolognini, "Vortex metrology by using Fourier analysis techniques: vortex networks correlation fringes," Appl. Opt. **51**, 7411–7419 (2012).
8. W. Wang, S. G. Hanson, and M. Takeda, "Optical vortex metrology," in *Advances in Speckle Metrology and Related Techniques*, G. H. Kaufmann, ed. (Wiley-VCH, 2011), Chap. 5, pp. 207–238.
9. W. Wang, T. Yokozeki, R. Ishijima, A. Wada, Y. Miyamoto, M. Takeda, and S. G. Hanson, "Optical vortex metrology for nanometric speckle displacement measurement," Opt. Express **14**, 120–127 (2006).
10. W. Wang, T. Yokozeki, R. Ishijima, and M. Takeda, "Optical vortex metrology based on the core structures of phase singularities in Laguerre–Gauss transform of a speckle pattern," Opt. Express **14**, 10195–10206 (2006).
11. P. Senthilkumaran, "Optical phase singularities in detection of laser beam collimation," Appl. Opt. **42**, 6314–6320 (2003).
12. J. W. Goodman, *Introduction to Fourier Optics*, 3rd ed. (Roberts, 2005), Chap. 4.
13. L. Angel-Toro, M. Tebaldi, M. Trivi, and N. Bolognini, "Properties of speckle patterns generated through multiaperture pupils," Opt. Commun. **192**, 37–47 (2001).